

Bid2X: Revealing Dynamics of Bidding Environment in Online Advertising from A Foundation Model Lens

Jiahao Ji*
Alibaba Group
Beijing, China

Tianyu Wang
Alibaba Group
Beijing, China

Yeshu Li
Alibaba Group
Beijing, China

Yusen Huo
Alibaba Group
Beijing, China

Zhilin Zhang
Alibaba Group
Beijing, China

Chuan Yu
Alibaba Group
Beijing, China

Jian Xu[†]
Alibaba Group
Beijing, China

Bo Zheng
Alibaba Group
Beijing, China

Abstract

Auto-bidding is crucial in facilitating online advertising by automatically providing bids for advertisers. While previous work has made great efforts to model bidding environments for better ad performance, it has limitations in generalizability across environments since these models are typically tailored for specific bidding scenarios. To this end, we approach the scenario-independent principles through a unified function that estimates the achieved effect under specific bids, such as budget consumption, gross merchandise volume (GMV), page views, etc. Then, we propose a bidding foundation model Bid2X to learn this fundamental function from data in various scenarios. Our Bid2X is built over uniform series embeddings that encode heterogeneous data through tailored embedding methods. To capture complex inter-variable and dynamic temporal dependencies in bidding data, we propose two attention mechanisms separately treating embeddings of different variables and embeddings at different times as attention tokens for representation learning. On top of the learned variable and temporal representations, a variable-aware fusion module is used to perform adaptive bidding outcome prediction. To model the unique bidding data distribution, we devise a zero-inflated projection module to incorporate the estimated non-zero probability into its value prediction, which makes up a joint optimization objective containing classification and regression. The objective is proven to converge to the zero-inflated distribution.

Our model has been deployed on the ad platform in Taobao, one of the world's largest e-commerce platforms. Offline evaluation on eight large-scale real-world datasets exhibits Bid2X's superiority

compared to various baselines and its generality across different scenarios. In real-world applications, Bid2X increased GMV by 4.65% and ROI by 2.44% in online A/B tests, paving the way for the bidding foundation model in computational advertising.

CCS Concepts

• Information systems → Computational advertising.

Keywords

Bidding environment modeling, Foundation model, Auto-bidding

ACM Reference Format:

Jiahao Ji, Tianyu Wang, Yeshu Li, Yusen Huo, Zhilin Zhang, Chuan Yu, Jian Xu, and Bo Zheng. 2025. Bid2X: Revealing Dynamics of Bidding Environment in Online Advertising from A Foundation Model Lens. In *Proceedings of the 31st ACM SIGKDD Conference on Knowledge Discovery and Data Mining V.2 (KDD '25)*, August 3–7, 2025, Toronto, ON, Canada. ACM, New York, NY, USA, 12 pages. <https://doi.org/10.1145/3711896.3737197>

1 Introduction

With the increasing automation of online advertising platforms, auto-bidding services (*i.e.*, automatically adjust bids for each ad impression) have become indispensable tools for advertisers to achieve ad performance goals in various advertising scenarios [24, 35, 39, 45]. On designing auto-bidding algorithms for e-commerce advertising, it is crucial to have a thorough understanding of the current bidding environment [12, 32]. Specifically, for an ad campaign, given a specific bid at a certain time slot, how much revenue will the advertiser earn and what is the total cost to pay for the revenue? Capturing such dynamic bidding environments can aid in responding more timely and accurately to changes in the marketplace, resulting in better ad performance [40].

Existing auto-bidding algorithms usually model the bidding environment implicitly, having limitations in comprehensively understanding the bidding environment and generalizing across environments. For example, linear programming (LP) computes the maximum total value of the impressions obtainable for a given bid based on historical bidding environments [10, 13, 51, 52]. Proportional–Integral–Derivative (PID) [7] based methods portray the

*This work was done during the internship at Alibaba Group.

[†]Corresponding author: xiyu.xj@alibaba-inc.com.

Permission to make digital or hard copies of all or part of this work for personal or classroom use is granted without fee provided that copies are not made or distributed for profit or commercial advantage and that copies bear this notice and the full citation on the first page. Copyrights for components of this work owned by others than the author(s) must be honored. Abstracting with credit is permitted. To copy otherwise, or republish, to post on servers or to redistribute to lists, requires prior specific permission and/or a fee. Request permissions from permissions@acm.org.
KDD '25, August 3–7, 2025, Toronto, ON, Canada.

© 2025 Copyright held by the owner/author(s). Publication rights licensed to ACM.
ACM ISBN 979-8-4007-1454-2/25/08
<https://doi.org/10.1145/3711896.3737197>

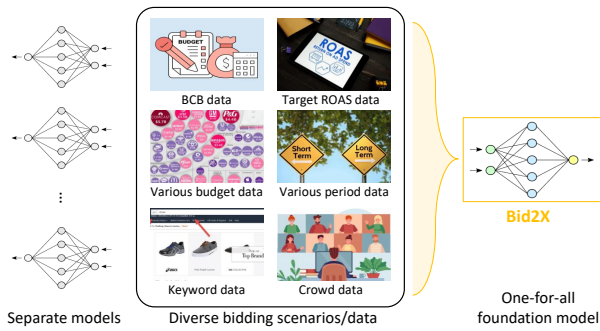


Figure 1: Existing models are designed and trained for specific bidding scenarios, so they cannot adapt to various scenarios. In contrast, we propose to train a one-for-all foundation model on broad bidding data, enabling it to handle a wide range of bidding scenarios.

possible cost for a given bid [11, 30, 44]. Reinforcement learning-based methods typically employ an environment model to learn the relation between the bid and cost or reward [4, 31]. These environment modeling processes can be summarized as a unified environment function $f_{\theta}(Y|bid_t)$, where Y involves target variables such as cost, reward, and count of the winning impressions, and t denotes the timestamp. Although these approaches depict bidding environments from different perspectives, none of them can provide a comprehensive description of the bidding environments. Moreover, as in Fig. 1, existing models are usually designed and trained for specific scenarios [4, 30, 51], lacking adaptability to new bidding scenarios and versatility across scenarios.

To overcome these problems, we propose to train a bidding foundation model, which is supposed to be “a large deep learning model trained on broad bidding environment data such that it can be applied across a wide range of bidding scenarios”. The bidding foundation model is versatile across various scenarios due to the existence of generalized principles that are independent of specific bidding environments. For example, more cost-effective impressions bring better ad performance, there exist closeness and periodicity in bidding environments, and the bid and its outcome follow the law of diminishing marginal returns.

However, it remains open to both academia and industry on how to build a bidding foundation model for industrial e-commerce advertising. We consider three challenges in this direction. (1) **Heterogeneous bidding data.** Data collected from different bidding scenarios lack uniformity and primarily consist of point data without temporal information, time series data, as well as discrete data and continuous data. Each type of data has its own characteristics, and there is currently no unified method to encode all of them. (2) **Complex and dynamic data dependency.** The real-world bidding environment is a highly dynamic multi-intelligence game process, which leads to complex dependencies between the control variable (bid) and target variables (cost, reward, count) in bidding data. Furthermore, these dependencies evolve with time, e.g., the same bid may bring more rewards at night than during working hours because people are more likely to shop online after work. Existing methods mainly learn dependencies between variables but

fail to consider temporal dynamics. (3) **Unique data distribution.** As engaging in the bidding process does not guarantee winning impressions, the bidding data often include many zero values, resulting in a zero-inflated distribution [21]. This unique distribution violates the normal data distribution assumption of existing neural network models, resulting in sub-optimal performance.

To address these challenges, we propose a bidding foundation model coined Bid2X, which leverages a conditional next-token prediction approach to learn universal principles from diverse bidding data across scenarios. **First**, we process different types of bidding data to encode them as uniform series representations, which provides input for dependency modeling. **Second**, to model complex and dynamic dependencies, we apply attention mechanisms to variable and temporal dimensions to learn the correlations from both perspectives. Then, we design a variable-aware fusion module to refine the inter-variable dependencies (learned from historical bidding data) with the bidding series of the day of interest. This provides a more accurate reference for the day’s bidding outcome prediction and improves our model’s adaptability to the day’s dynamic dependencies. **Third**, to model the unique distribution of bidding data, we devise an end-to-end zero-inflated projection module that combines the model’s prediction of the probability of a non-zero value and the magnitude of that value into a joint optimization objective. Moreover, we theoretically demonstrate that this objective can converge to the real distribution of bidding data under mild assumptions. Our contributions are four-fold:

- We introduce the novel concept of the bidding foundation model for bidding environment modeling, marking a significant innovation in the field of computational advertising. This paradigm innovation moves beyond the limitations of traditional, scenario-specific models and provides a solution capable of generalizing across various bidding environments.
- We for the first time identify three unique challenges of the bidding environment modeling problem, which are fundamental to developing bidding foundation models and advancing the capability of computational advertising systems.
- We propose a bidding foundation model Bid2X that can unify heterogeneous bidding data as series embedding and learn complex and dynamic dependencies to achieve generalization across environments. We theoretically ensure that the model can converge to the zero-inflated data distribution.
- Extensive experiments on eight real-world datasets demonstrate the superior generalization of Bid2X in various scenarios compared to several baselines. Online results in Taobao, a large e-commerce company, further verify our model’s effectiveness.

2 Related Work

Auto-bidding and Bidding Environment Modeling. Auto-bidding techniques in computational advertising have been a research focus in recent years [29, 35, 45]. They are employed to automatically place bids on ad spaces, offering convenience and efficiency in managing bids compared to manual bidding. The main focus of such techniques is to optimize given key performance indicators (e.g., clicks or conversions) while maintaining a certain budget [12, 39]. A straightforward solution for auto-bidding is linear programming based on the historical bidding environment [10, 13, 24, 51, 52].

While it is highly efficient and simple to implement, it does not take the dynamic nature of the bidding environment into account. To model such dynamics, some work utilizes the PID algorithm from the control theory [7] to adjust the bidding strategy based on the latest observed data. Some typical examples are shown in [11, 30, 44], which aim to control different variables such as cost-per-click, budget pacing, etc. These controlling methods enable the bidding agents to perceive the current environment in real time and then update the bids that were once based on outdated data [32]. Recently, reinforcement learning (RL) based methods have emerged as a promising approach due to their ability to effectively handle the sequential nature of the bidding process [13, 16, 48]. For example, Cai et al. [4] designed a bidding environment and applied a deep RL algorithm to learn the optimal bidding strategy. Zhang et al. [31] adopted the RL framework for auto-bidding and showed that their approach can outperform traditional bidding strategies. In addition, landscape forecasting methods [22, 34] that predict the probability distribution of market prices for each advertising auction can also be regarded as bidding environment modeling methods, but they do not directly predict bidding results. However, these methods are usually designed for specific scenarios and cannot be well generalized across various bidding scenarios.

Foundation Model. Foundation models are general-purpose technologies that can support a diverse range of scenarios [2]. Typically, they are large deep-learning models trained on broad and massive data. They have been developed across a range of modalities, such as text [47], vision [1], graph [25], time series [23], and even robotics [9] and autonomous driving [5]. However, the foundation model in computational advertising has rarely been explored.

Time Series Prediction. Time series prediction (TSP) aims to fit a model using historical (time-stamped) data to predict future values of variables. It is crucial in fields like epidemiology [38], transportation [17–20, 37], and meteorology [14]. Extensive research has been conducted in both traditional statistics [3, 15] and deep learning [33, 36]. Recent studies have seen a surge in Transformer-based TSP models [27, 41, 42, 46, 49, 50], which can be categorized into two groups: temporal-wise and variable-wise. The former builds input tokens from series values at each time slot, which has been widely researched [46, 49]. However, these studies are confronted with issues like timestep mixing and permutation invariance, leading to underperformance on some datasets compared to simple linear predictors [27, 43]. To tackle this, variable-wise Transformers that consider series data of each variable as a token are proposed and show the state-of-the-art performance in TSP. However, these methods have not yet been explored in the bidding environment modeling problem and we make the first attempt.

3 Preliminaries

In this section, we first define some basic concepts and then introduce the studied problem of this paper.

Definition 1 (Ad Campaign). *An ad campaign C is an order in which an advertiser seeks product promotion constrained by budget, product category, advertiser category, and delivery start/end times. It also involves some contextual information such as total historical clicks, total historical costs, total historical cost effectiveness, etc.*

In online advertising platforms, an ad campaign is usually settled and reset at the end of each day. Therefore, we denote the i -th ad campaign at day τ as $C_i^{(\tau)}$.

Definition 2 (Bidding Trajectory). *A bidding trajectory is a sequence of bidding records generated in the execution process of an ad campaign $C_i^{(\tau)}$, denoted as $X_i^{(\tau)} = (x_{i,1}^{(\tau)}, \dots, x_{i,m}^{(\tau)})$, where m is the number of bidding records. Each record $x = (b, c, r, ct, t)$, where b is the bid, c , r , and ct represent the cumulative cost, reward, and count of winning impressions over the time from timestamp t to the time when the bid is adjusted respectively. We call a bidding trajectory **complete** when the corresponding ad campaign is finished, otherwise it is **incomplete**.*

Note that in a bidding record, b is the optimal bidding parameter introduced in [13], which can be transformed into the real bid. In general, one day is divided into several time slots (ticks) according to the minimum bid adjustment period. Accordingly, we can map each bid record into a time slot. We observe that some time slots have no bidding record, and a bidding trajectory does not necessarily start from the first time slot and end at the last time slot.

Definition 3 (Bidding Environment Modeling Problem). *Given historical bidding data $\{X_i^{(\tau-1)}, C_i^{(\tau-1)}\}$, today's bidding data until time slot t , i.e., $\{X_i^{(\tau)}, C_i^{(\tau)}\}$, and bid information $b_{i,t+1}^{(\tau)}$ of the next time slot $t+1$, the **bidding environment modeling problem** aims to predict the corresponding outcomes via a function $f_{\Theta}(\cdot)$:*

$$\mathbf{y}_{i,t+1}^{(\tau)} = f_{\Theta}(b_{i,t+1}^{(\tau)}, X_i^{(\tau)}, C_i^{(\tau)}, X_i^{(\tau-1)}, C_i^{(\tau-1)}), \quad (1)$$

where the output includes the cost, reward, and count at the $(t+1)$ -th time slot, i.e., $\mathbf{y}_{i,t+1}^{(\tau)} = (c_{i,t+1}^{(\tau)}, r_{i,t+1}^{(\tau)}, ct_{i,t+1}^{(\tau)})$.

We leverage the temporal nature of the data and frame the bidding environment modeling problem as a self-supervised task that predicts the most likely outcome at the next time step (given a bid) based on previous bidding records, i.e., conditional next-token prediction. Our problem formulation does not require manual annotations, as both the input and target are inherently present in the data, akin to how they are in language data. This novel self-supervised problem formulation approach facilitates effectively capturing the temporal dynamics of the bidding environment and paves the way for foundation models in this domain.

It is worth noting that in Definition 3 the historical bidding trajectories are complete whereas today's bidding trajectories are still in progress. Therefore, we utilize the historical trajectory to learn the complex correlations among different variables (e.g., bid and cost) and today's incomplete trajectory to capture the dynamic temporal dependency. To avoid clutter of notations, we omit the sample index i for all symbols in the rest of this paper.

4 Method

In this section, we give a detailed introduction of the proposed Bid2X foundation model with illustration in Fig. 2. First, we provide a unified data embedding method for heterogeneous bidding data in Section 4.1. Then, we elaborate on the bidding transformer used for variable and temporal dependency modeling in Section 4.2. Finally, we detail a zero-inflated projection for the unique distribution of bidding data, and introduce a self-supervised auxiliary task to complement information from a global view in Section 4.3.

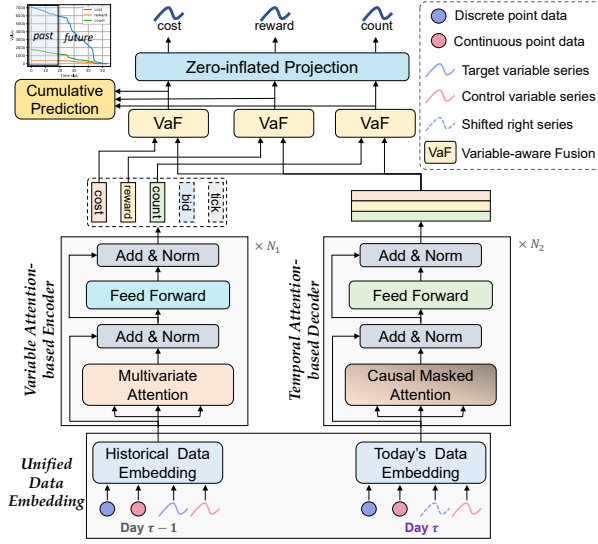


Figure 2: The overall architecture of our Bid2X model.

4.1 Unified Data Embedding

This part aims to transform heterogeneous bidding data into a unified series embedding with tailored embedding methods. Since historical data and today’s data are used for modeling different types of dependencies, we embed them via separate modules.

Historical Data Embedding. Historical data are utilized for inter-variable correlation modeling, so we propose to transform each variable series into an independent embedding.

Specifically, given the cost series $\mathbf{c}^{(\tau-1)} = (c_1^{(\tau-1)}, \dots, c_{T_{\tau-1}}^{(\tau-1)})$ of trajectory $\mathbf{X}^{(\tau-1)}$ with length $T_{\tau-1}$, we encode it as $\mathbf{z}_c^{(\tau-1)} \in \mathbb{R}^D$ via

$$\mathbf{z}_c^{(\tau-1)} = \mathbf{c}^{(\tau-1)} \cdot \mathbf{W}_c^\top, \quad (2)$$

where $\mathbf{W}_c \in \mathbb{R}^{D \times T_{\tau-1}}$ is learnable parameters. Since different bidding trajectories have different lengths, we pad all trajectories to the maximum length T . The shape of \mathbf{W}_c is therefore $D \times T$. Similar to the cost series, we can generate embeddings of other variables. By using these embeddings, we can form an embedding matrix $\bar{\mathbf{Z}}_s^{(\tau-1)} \in \mathbb{R}^{C_0 \times D}$, where C_0 is the number of input variables.

Besides the series data, there is some constraint and context information in ad campaign data $\mathbf{C}^{(\tau-1)}$, including discrete and continuous data. For the discrete one-hot categorical constraints such as the advertiser category, an embedding layer is used to transform them into low-dimensional dense representations. For the j -th categorical constraint t_j , let $\mathbf{E}^{(j)} = (\mathbf{e}_1^{(j)}, \dots, \mathbf{e}_{K_j}^{(j)})^\top \in \mathbb{R}^{K_j \times D}$ represent the j -th embedding dictionary, where $\mathbf{e}_k^{(j)} \in \mathbb{R}^D$ is an embedding vector with dimensionality of D . The embedding operation follows the table lookup mechanism, i.e., if the i -th entry of t_j is $t_{j,i} = 1$, the embedded representation of t_j is a single embedding vector $\mathbf{e}_i^{(j)}$. For the continuous numeric constraints like budget, we separately feed each constraint into different linear transformations to generate embedding. The same transformation is employed for context data as they are all numeric features. Next, all ad campaign embeddings are summed as a single context embedding $\bar{\mathbf{Z}}_c^{(\tau-1)} \in \mathbb{R}^D$.

Finally, we sum up the variable embedding $\bar{\mathbf{Z}}_s^{(\tau-1)}$ and the context embedding $\bar{\mathbf{Z}}_c^{(\tau-1)}$ to produce the historical data embedding via

$$\mathbf{Z}^{(\tau-1)} = \bar{\mathbf{Z}}_s^{(\tau-1)} \oplus \bar{\mathbf{Z}}_c^{(\tau-1)}, \quad (3)$$

where \oplus is the broadcasting addition operation, which first duplicates the lower-dimensional matrix to match the shape of the higher-dimensional matrix and then adds them together.

Today’s Data Embedding. Today’s data are utilized for temporal dependency modeling, so we treat all values of a time slot as a token and encode them as a D -dimensional embedding.

Before delving into the embedding layer, we preprocess the bidding trajectory to avoid information leakage and facilitate modeling convenience. Specifically, given bidding trajectory until the current time slot t : $\mathbf{X}^{(\tau)} = (\mathbf{x}_1^{(\tau)}, \dots, \mathbf{x}_t^{(\tau)}) \in \mathbb{R}^{C_0 \times t}$, we split it into two parts along the variable dimension C_0 : $\mathbf{X}_p^{(\tau)} \in \mathbb{R}^{C_1 \times t}$ that contains control variables (bid and tick time) and $\mathbf{X}_q^{(\tau)} \in \mathbb{R}^{C_2 \times t}$ that contains target variables (cost, reward, and count). To avoid information leakage, we shift right the target series and use a zero vector as the start token, making $\mathbf{X}_p^{(\tau)} = (\mathbf{0}, \mathbf{x}_{p,1}^{(\tau)}, \dots, \mathbf{x}_{p,t}^{(\tau)})$. Meanwhile, we include the future bid information at the end of the control series, making $\mathbf{X}_q^{(\tau)} = (\mathbf{x}_{q,1}^{(\tau)}, \dots, \mathbf{x}_{q,t}^{(\tau)}, \mathbf{x}_{q,t+1}^{(\tau)})$. Then, we stack these two series back to the original format and obtain $\mathbf{X}^{(\tau)} \in \mathbb{R}^{C_0 \times (t+1)}$. It is further padded to the max length T along the time dimension $t+1$ for computational convenience because different bidding trajectories have different lengths, resulting in the input shape $C_0 \times T$.

Based on the preprocessed bidding trajectory $\mathbf{X}^{(\tau)} \in \mathbb{R}^{C_0 \times T}$, we transform the t' -th token $\mathbf{x}_{t'}^{(\tau)} \in \mathbb{R}^{C_0}$ as

$$\mathbf{z}_{t'}^{(\tau)} = \mathbf{x}_{t'}^{(\tau)} \cdot \mathbf{W}_x^\top, \quad (4)$$

where $\mathbf{W}_x \in \mathbb{R}^{D \times C_0}$. By applying the transformation to all time slots, we can obtain an embedding $\bar{\mathbf{Z}}_s^{(\tau)} \in \mathbb{R}^{T \times D}$. This embedding involves the global timestamp by a learnable time embedding in control variables, but the local positional information of the tokens in the sequence is not preserved. To this end, we add positional encoding to $\bar{\mathbf{Z}}_s^{(\tau)}$ with a fixed position embedding matrix \mathbf{P} defined by $p_{i,2d} = \sin(i/(2T)^{2d/D})$ and $p_{i,2d+1} = \cos(i/(2T)^{2d/D})$.

By repeating the same process for campaign data $\mathbf{C}^{(\tau)}$ as that in the historical data embedding module, we can have a context representation $\bar{\mathbf{Z}}_c^{(\tau)} \in \mathbb{R}^D$. On top of this, we generate today’s data embedding as follows:

$$\mathbf{Z}^{(\tau)} = \bar{\mathbf{Z}}_s^{(\tau)} \oplus \bar{\mathbf{Z}}_c^{(\tau)}. \quad (5)$$

4.2 Bidding Transformer

This part aims to inject the complex inter-variable correlation into historical embedding $\mathbf{Z}^{(\tau-1)}$ and dynamic temporal dependency into today’s embedding $\mathbf{Z}^{(\tau)}$ with two attention mechanisms. Then, we fuse $\mathbf{Z}^{(\tau-1)}$ and $\mathbf{Z}^{(\tau)}$ for a comprehensive understanding of bidding environments by a variable-aware fusion module.

4.2.1 Variable Attention-based Encoder. We first model the complex correlation between different variables (e.g., bid and cost, bid and reward, etc.) with a variable attention mechanism, where the model treats each variable as a token and learns pairwise variable relationships. Specifically, given historical embedding $\mathbf{Z}^{(\tau-1)} \in \mathbb{R}^{C_0 \times D}$, we map it into $\mathbf{Q}^{(\tau-1)}, \mathbf{K}^{(\tau-1)}, \mathbf{V}^{(\tau-1)} \in \mathbb{R}^{C_0 \times D}$ by three linear projections. Let $\mathbf{q}_m^{(\tau-1)}, \mathbf{k}_n^{(\tau-1)}$ stand for the m -th and n -th row

in $\mathbf{Q}^{(\tau-1)}$, $\mathbf{K}^{(\tau-1)}$ respectively. We can compute the correlation between the m -th and n -th variables by

$$\alpha_{m,n} = \frac{\exp\left(\left(\mathbf{q}_m^{(\tau-1)}\right)^\top \cdot \mathbf{k}_n^{(\tau-1)} / \lambda\right)}{\sum_{n'=1}^{C_0} \exp\left(\left(\mathbf{q}_m^{(\tau-1)}\right)^\top \cdot \mathbf{k}_{n'}^{(\tau-1)} / \lambda\right)}, \quad (6)$$

where λ is the scale factor and is set to \sqrt{D} . By calculating all $\alpha_{m,n}$, we can have a variable correlation map $\mathbf{A} \in \mathbb{R}^{C_0 \times C_0}$ that exhibits the multivariate correlations between paired variables. Consequently, highly correlated variables will be more weighted for the next representation interaction with $\mathbf{V}^{(\tau-1)}$. The interaction is formulated as $\text{LN}(\mathbf{Z}^{(\tau-1)} + \mathbf{A} \cdot \mathbf{V}^{(\tau-1)})$, where LN denote layer normalization. After that, all variables' representations are independently processed by a shared feed-forward network, which aims to portray the intrinsic properties of every variable, such as the amplitude and trend. The above modules make up a variable-based attention block. By stacking N_1 such blocks, we obtain the output representation $\mathbf{H}^{(var)} \in \mathbb{R}^{C_0 \times D}$ that fully captures the inter-variable correlation.

4.2.2 Temporal Attention-based Decoder. Apart from the inter-variable correlation, the temporal dependency evolving with time is also an important perspective of bidding environments. We capture such dynamic dependency along the temporal dimension with a causal attention mechanism, where the model treats each time slot as a token and only attends to tokens in the past. Specifically, given today's embedding $\mathbf{Z}^{(\tau)} \in \mathbb{R}^{T \times D}$, we generate queries, keys, and values as $\mathbf{Q}^{(\tau)}$, $\mathbf{K}^{(\tau)}$, $\mathbf{V}^{(\tau)} \in \mathbb{R}^{T \times D}$ for attention computation. The temporal attention map $\mathbf{B} \in \mathbb{R}^{T \times T}$ is then computed as

$$\mathbf{B} = \text{Softmax}\left(\frac{\mathbf{Q}^{(\tau)} \cdot (\mathbf{K}^{(\tau)})^\top}{\sqrt{D}} \odot \mathbf{M}\right), \quad (7)$$

where $\mathbf{M} = \mathbf{L}_1 + \mathbf{U}_{-\text{inf}} \in \mathbb{R}^{T \times T}$ is the causal masking matrix with \mathbf{L}_1 a one-valued lower triangular matrix and $\mathbf{U}_{-\text{inf}}$ a ($-\text{inf}$)-valued strict upper triangular matrix. The masking matrix leads to \mathbf{B} a lower triangular matrix in which all the entries above the main diagonal are zero. This ensures no information leakage during temporal dependency learning because our model only attends to past information and cannot see future ones. On top of the learned temporal attention map, the remaining operations are the same as those in the variable-based attention module. After these operations, we can obtain output representation $\mathbf{H}^{(tem)} \in \mathbb{R}^{T \times D}$ that captures the dynamic temporal dependency in bidding trajectories.

4.2.3 Variable-aware Fusion. To make the model better understand the complex bidding environment, we fuse the representations from the variable and temporal perspectives. Since different variables describe the bidding environment from different views, we propose a Variable-aware Fusion (VaF) method to preserve environment diversity and enhance our model's robustness.

Specifically, given variable representation matrix $\mathbf{H}^{(var)}$, we extract the target variables' representations as $\mathbf{H}_p^{(var)} \in \mathbb{R}^{C_2 \times D}$ and iteratively utilize each row to generate fused representation. Let $\mathbf{h}_i^{(var)} \in \mathbb{R}^D$ be the representation of the i -th target variable. We fuse it with the temporal representation matrix $\mathbf{H}^{(tem)} \in \mathbb{R}^{T \times D}$ via

$$\mathbf{H}_i = \sigma(\hat{\mathbf{H}}_i) \odot \mathbf{H}^{(tem)}, \quad (8)$$

where \odot denotes the element-wise Hadamard product. The sigmoid gate $\sigma(\hat{\mathbf{H}}_i)$ controls which input $\mathbf{H}^{(tem)}$ is relevant for forecasting

future states of the i -th target variable. Its input $\hat{\mathbf{H}}_i$ is produced by $\hat{\mathbf{H}}_i = \text{MLP}\left(\text{Concat}\left(\mathbf{h}_i^{(var)}, \mathbf{H}^{(tem)}\right)\right)$, where MLP is a two-layer fully connected network, and Concat represents the concatenation operation with broadcasting.

Remark: The two attention mechanisms we designed in the bidding transformer can depict bidding environments from the perspective of variables and time respectively, thus providing a fine and complete description of their dynamics. Moreover, when the environment changes, variable attention can function as a context learner to perceive the new dependency between variables. This can enhance our model's ability to adapt to new environments, which is empirically verified in Section 6.2 and 6.4.1.

4.3 Zero-inflated Projection & Auxiliary Task

4.3.1 Zero-inflated Projection. To model the unique zero-inflated distribution of bidding data, we enable our model to be aware of the zero information by a binary classifier and incorporate such information into the prediction of bidding results for joint optimization.

Specifically, given the embedding of the i -th target variable \mathbf{H}_i , we estimate the probability of the target value y_i not be zero via

$$\Pr(y_i \neq 0) = \sigma(\text{MLP}(\mathbf{H}_i)), \quad (9)$$

where $\sigma(\cdot)$ is the sigmoid function. On top of this, we produce the value prediction by incorporating the non-zero probability:

$$\hat{y}_i = \Pr(y_i \neq 0) \cdot \tilde{y}_i + (1 - \Pr(y_i \neq 0)) \cdot 0, \quad (10)$$

where $\tilde{y}_i = \text{MLP}(\mathbf{H}_i)$ is the prediction of the target value's magnitude. Since it takes into the zero-inflated phenomenon while projecting the target variable, we name it "zero-inflated projection".

Finally, we can derive a joint optimization objective that combines cross entropy (CE) loss and mean square error (MSE) loss:

$$\mathcal{L}_i^{(z)} = \underbrace{\Pr(y_i \neq 0) \cdot I_{\{y_i \neq 0\}} + (1 - \Pr(y_i \neq 0)) \cdot I_{\{y_i = 0\}}}_{\text{CE}} + \underbrace{(y_i - \hat{y}_i)^2}_{\text{MSE}}, \quad (11)$$

where $I_{\{\cdot\}}$ is the indicator function. This joint objective allows the model predictions to converge to the zero-inflated distribution, with a theoretical guarantee provided in Section 5 and empirical evaluation in Appendix E. By adding the loss function of all C_2 target variables, we obtain the overall loss for zero-inflated projection:

$$\mathcal{L}^{(z)} = \sum_{i=1}^{C_2} \mathcal{L}_i^{(z)}. \quad (12)$$

Existing studies for zero-inflated distribution usually take a two-step paradigm, where the first step trains a classifier to determine whether the target value is zero and the second trains a projector for only non-zero values [6]. The performance of these methods is limited by the classifier, which estimates a hard binary label for each sample. Consequently, if the classifier predicts non-zero samples with zero labels, the projector will be disabled, leading to large prediction errors. In contrast, our model takes an end-to-end approach that estimates a soft label $\Pr(y_i \neq 0)$ for each sample. It can work together with the predictor to control the final predicted value. This allows the predictor to correct its forecast when the classifier's prediction is not up to standard. Additionally, this comprehensive approach streamlines the model training process.

4.3.2 Cumulative Prediction. To give our model a global view of bidding environments, we propose a self-supervised auxiliary task that forecasts future cumulative information using the target variable representation, as in the upper left part of Fig. 2.

Specifically, given the i -th target variable’s representation H_i , we predict the cumulative value from the current time slot to the end of the ad campaign of the target variable by

$$\hat{y}_i^{(c)} = \text{MLP}(H_i), \quad (13)$$

where $\hat{y}_i^{(c)}$ is the prediction result. With its ground truth $y_i^{(c)}$, we can optimize this task by a mean square error loss:

$$\mathcal{L}^{(c)} = \sum_{i=1}^{C_2} \left(\hat{y}_i^{(c)} - y_i^{(c)} \right)^2. \quad (14)$$

4.3.3 Model Training. Based on the zero-inflated projection loss in Eq. (12) and cumulative prediction loss in Eq. (14), we can obtain the overall optimization objective as follows:

$$\mathcal{L} = \mathcal{L}^{(z)} + \gamma \mathcal{L}^{(c)}, \quad (15)$$

where γ is a balancing factor. With loss \mathcal{L} , our model can be trained by the backpropagation algorithm in an end-to-end manner.

5 Theoretical Analysis

In order to study the theoretical properties of the proposed zero-inflated projection loss, we consider a more general supervised learning setting where we are interested in learning a mapping $f : \mathbb{R}^d \rightarrow \mathbb{R}$ given empirical data $\{\mathbf{x}, \mathbf{y}\}_{i=1}^m$ with $\mathbf{x} \in \mathbb{R}^d$ and $\mathbf{y} \in \mathbb{R}$. Similar to Eq. (10), we define a zero-inflated model [6] for Y , in which the expectation can be written as

$$\mathbb{E}[Y|\mathbf{x}] \triangleq p(\mathbf{x}) \cdot g(\mathbf{x}) + (1 - p(\mathbf{x})) \cdot 0, \quad (16)$$

where p is the true probability of Y being in the non-negative group and g is a deterministic function standing for the non-negative ground-truth expected label. We propose the following optimization objective:

$$\min_{\theta, \phi} \mathcal{L} := \mathbb{E}_{(\mathbf{X}, Y) \sim \mathbb{P}} (p_\theta(\mathbf{X})g_\phi(\mathbf{X}) - Y)^2 + H(p(\mathbf{X})|p_\theta(\mathbf{X})),$$

where $H(p|p_\theta) = -p \ln p_\theta - (1 - p) \ln (1 - p_\theta)$ is the binary cross entropy between p and p_θ .

We next show that the learned conditional label distribution converges to the true distribution in the true-data setting.

Theorem 4 (Zero-inflated Proper Loss). *Let \mathcal{F} be a set of all measurable functions and $p_\theta, g_\phi \in \mathcal{F}$. Assume that p and g are conditionally independent, then, with respect to the zero-inflated model defined in Eq. (16), we have $p_{\theta^*}(\mathbf{x}) = p(\mathbf{x})$ and $p_{\theta^*}(\mathbf{x})g_{\phi^*}(\mathbf{x}) = p(\mathbf{x})g(\mathbf{x})$, therefore $f(\mathbf{x}) = \mathbb{E}[Y|\mathbf{x}]$ for any $\mathbf{x} \in \mathbb{R}^d$. In addition, $g_{\phi^*}(\mathbf{x})$ is generally not unique.*

To be brief, we show the consistency of the proposed loss by taking advantage of standard KKT conditions and implications of Hessian matrices with respect to convexity. We defer the detailed proof to Appendix A.

6 Experiments

6.1 Experimental Settings

6.1.1 Dataset & Baseline. To evaluate the performance of Bid2X, we conduct extensive experiments on eight ad bidding datasets

containing 132,734,218 bidding trajectories and 3,070,868 bidding records from the advertising platform in Taobao, one of the largest e-commerce platforms worldwide. The datasets cover multiple types of bidding strategies (e.g., BCB [51], TargetROAS [8]), spanning various advertisers with various budgets and delivery durations. Tab. 5 and Tab. 6 in Appendix B summarize the datasets, illustrating diversity across scenarios.

We choose Mean Average Error (MAE) and Root Mean Square Error (RMSE) for performance evaluation. A lower metric value indicates better performance. The baselines we compare can be divided into four streams. *i) Landscape forecasting approaches* model the market competition in online advertising by forecasting the probability distribution of market price for each ad auction. The compared models includes DLF [34] and ADM [22]. We adapt them by feeding the hidden representations before the final prediction layers into an MLP for bid outcome prediction. *ii) Heuristic method* includes historical log-based LP [13]. *iii) Variable-based approaches* aims to model the relations between bid and its outcomes, including MMP [26] and MLP [12] that consider variable relations at bid record level, and iTransformer [27] considering relation at the bidding trajectory level. *iv) Temporal-based approaches* mainly consider the dynamic sequence dependency of different bid records in a bidding trajectory. The compared baselines include non-stationary transformer (NST) [28] and Informer [49]. For a fair comparison, we also train Informer for all datasets in a foundation-model manner, denoted as Informer(fm).

6.1.2 Implementation Protocol. Our Bid2X is implemented with PyTorch 2.2.0 with an NVIDIA L40S GPU. The number of layers is set to 2. The hidden dimension D is searched from 32 to 1024. For the task balancing factor γ , we test it from $\{0.5, 0.75, 1, 1.25, 1.5\}$. Our model is trained using Adam optimizer with a learning rate of 0.0001 and batch size of 128. The final parameter setting of our model is according to Fig. 6 in Appendix D.

6.2 Overall Performance

We split every dataset into training, validation, and test sets in a ratio of 1:1:1. For baselines, we train a dedicated model for each dataset, while Bid2X is trained and evaluated across all datasets in a one-for-all foundation paradigm. Tab. 1 presents the comparison results of the environment modeling task. We have the following key findings: **(1)** Bid2X outperforms all competing baselines across every target variable on eight datasets with a large margin. This underscores the significant potential and benefits of our bidding foundation model where different datasets can benefit each other for learning generalized bidding laws. **(2)** Baseline approaches exhibit inconsistent performance across diverse datasets, indicating their instability across scenarios. In contrast, our model consistently offers more stable and reliable results, highlighting its robustness and adaptability to various bidding scenarios. **(3)** Interestingly, Informer(fm) performs worse than baselines dedicated for each dataset in some cases, suggesting that Informer struggles to adapt to these distinct data distributions relying solely on temporal dependency modeling. **(4)** Approaches that focus on modeling the dynamic environment, whether variable or temporal-based models, generally outperform heuristic methods that rely on a stationary assumption of the current and historical environment. This reflects

Table 1: Performance comparison over eight datasets in terms of MAE and RMSE w.r.t. three target variables: cost, reward, count. “-” means the model cannot produce corresponding predictions. The bold/underlined font means the best/the second-best result.

Dataset	BCB		TR		BS		BM		BL		D6		D12		D18	
	MAE	RMSE	MAE	RMSE	MAE	RMSE	MAE	RMSE	MAE	RMSE	MAE	RMSE	MAE	RMSE	MAE	RMSE
DLF	177.22	1038.73	337.56	2288.56	188.69	435.47	1317.44	2364.62	7130.59	13144.37	386.03	1225.56	266.31	1026.17	233.19	998.94
ADM	164.26	992.28	279.40	1382.48	187.83	432.65	1222.74	2314.76	8492.74	15877.66	356.57	1168.13	249.72	907.07	201.67	837.37
LP	521.28	5513.79	670.94	5652.17	630.71	5551.63	2881.14	14380.97	16479.33	44689.66	626.78	6085.45	470.77	4992.03	458.36	4823.93
MMP	165.08	<u>792.29</u>	257.96	1195.95	199.92	471.19	1520.61	35308.12	11211.28	29587.71	218.11	971.93	151.22	803.43	131.16	724.20
MLP	<u>157.60</u>	814.94	223.84	<u>914.96</u>	184.27	<u>429.32</u>	<u>975.87</u>	<u>2040.10</u>	8427.86	16257.88	<u>198.76</u>	<u>832.21</u>	<u>139.27</u>	892.18	119.63	647.71
iTransformer	183.83	949.73	269.15	1278.51	207.98	487.07	1223.86	2467.54	7708.04	14322.90	243.03	1130.71	165.90	938.27	133.25	744.00
NST	161.79	965.66	234.83	1103.03	186.42	440.66	1057.50	2141.10	8222.52	14977.61	208.37	909.10	149.90	859.11	120.81	616.08
Informer	159.31	805.66	239.38	1141.87	<u>180.92</u>	450.02	1065.46	2220.36	7952.92	15233.91	209.18	944.01	145.15	803.10	120.96	664.25
Informer(fm)	158.55	796.40	<u>214.56</u>	1060.32	187.06	448.36	1015.16	2115.96	<u>6037.38</u>	<u>12460.79</u>	206.43	944.93	140.57	<u>759.19</u>	<u>113.55</u>	<u>607.79</u>
Bid2X(fm)	122.50	589.35	172.40	792.90	148.28	370.69	751.83	1618.24	4170.21	8758.04	158.81	717.49	109.27	553.85	88.96	425.67
DLF	8.15	58.33	12.80	162.93	16.23	66.72	64.07	286.65	281.75	1249.32	39.61	302.77	24.68	177.88	17.43	149.91
ADM	8.01	47.52	12.27	156.54	15.87	60.99	51.77	232.26	296.32	1366.17	30.95	273.44	21.25	145.96	14.21	124.81
LP	1532.06	23559.05	2077.69	42414.41	2006.52	25790.00	8094.40	61671.17	43145.00	303338.10	1905.18	25388.42	1415.57	29026.07	1155.66	22983.07
MMP	8.27	49.26	13.06	176.42	10.49	45.89	48.59	142.20	652.76	3698.89	10.97	62.07	7.54	99.03	5.71	43.97
MLP	8.12	47.84	<u>10.98</u>	<u>149.19</u>	9.96	42.50	42.14	<u>120.07</u>	294.89	1368.50	9.93	<u>52.17</u>	7.13	61.81	4.91	<u>32.87</u>
iTransformer	8.06	49.01	12.24	155.90	10.14	45.28	46.89	136.52	254.78	<u>1124.58</u>	10.85	62.31	7.34	89.07	5.21	41.63
NST	7.47	49.30	11.05	148.25	9.50	<u>41.65</u>	43.64	133.94	248.60	1156.04	10.63	305.18	7.45	271.76	4.97	38.05
Informer	7.46	<u>44.35</u>	11.64	170.88	9.55	42.63	42.98	127.11	295.86	1380.27	9.97	55.48	6.85	95.12	5.01	41.72
Informer(fm)	<u>7.44</u>	44.42	11.24	162.57	<u>9.42</u>	42.20	<u>42.05</u>	125.00	<u>233.72</u>	1252.80	<u>9.92</u>	56.18	<u>6.74</u>	<u>91.36</u>	<u>4.82</u>	38.12
Bid2X(fm)	5.94	35.28	8.90	131.92	7.76	35.65	31.91	99.01	170.03	999.59	7.82	44.63	5.45	74.23	4.01	27.68
DLF	22.04	104.71	28.73	144.89	52.10	167.94	122.49	326.37	475.95	1241.22	71.22	286.95	46.49	229.12	35.10	279.45
ADM	20.46	98.49	24.93	108.11	49.09	152.89	88.12	291.09	510.54	1263.78	47.42	242.83	35.47	194.74	28.81	227.71
LP	-	-	-	-	-	-	-	-	-	-	-	-	-	-	-	-
MMP	20.23	98.57	24.30	102.68	25.24	85.18	93.96	372.61	862.19	5439.32	23.90	114.03	17.99	87.49	17.41	86.01
MLP	18.54	<u>92.12</u>	20.70	92.02	<u>22.74</u>	78.46	75.29	274.30	302.62	750.63	22.87	109.58	<u>16.26</u>	<u>78.44</u>	16.95	79.97
iTransformer	21.75	103.70	24.91	104.19	26.75	88.34	91.51	302.15	290.17	713.01	25.96	118.74	19.47	92.26	17.64	85.13
NST	19.35	105.96	22.39	94.04	23.63	80.60	81.31	278.85	315.69	751.85	22.99	<u>107.69</u>	17.19	80.49	16.53	78.88
Informer	19.27	97.05	22.96	99.89	23.68	82.45	81.74	290.02	313.97	784.46	22.99	111.42	17.44	86.46	16.39	82.05
Informer(fm)	19.12	95.93	<u>20.38</u>	<u>91.81</u>	23.42	81.63	<u>73.92</u>	<u>267.62</u>	<u>246.93</u>	<u>672.31</u>	<u>22.60</u>	109.88	16.82	83.00	<u>15.38</u>	<u>77.00</u>
Bid2X(fm)	12.02	72.07	13.26	66.96	14.54	58.85	47.21	210.57	151.70	475.96	14.30	84.57	10.53	61.03	9.23	50.73

the importance of capturing environmental dynamics from both variable and temporal perspectives.

6.3 Zero-Shot Performance

The remarkable feature of the foundation model is its excellent generalizability. Few-shot and zero-shot generalizations are often used as the ultimate task to assess this ability. To this end, we evaluate our Bid2X through the few-shot learning and zero-shot generalization in this part. Specifically, we select a new dataset unseen by any model in Tab. 1 from the crowd-type bidding scenario. We split it into training, validation, and test sets in a ratio of 1:1:1. In few-shot learning, only a restricted amount of training data, namely 1% and 5%, are utilized for model learning. We compare our Bid2X with some competitive baselines. To increase the task difficulty, we also evaluate the zero-shot performance of Bid2X via direct testing without a training phase. Tab. 7 in Appendix C provides the full few-shot results. Due to limited space, we visualize the MAE result regarding the “cost” target variable in Fig. 3. As observed, Bid2X demonstrates a superior generalization performance over the baseline models. This generalization can be attributed to the successful transfer of learned variable relationships. This suggests

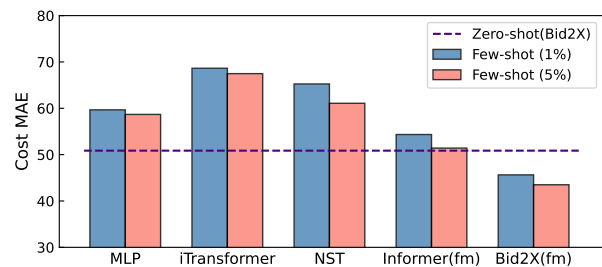


Figure 3: Few-shot performance of Bid2X and baselines on the crowd-type bidding scenario with 1% and 5% training data. Zero-shot results of our Bid2X are given by the dashed line.

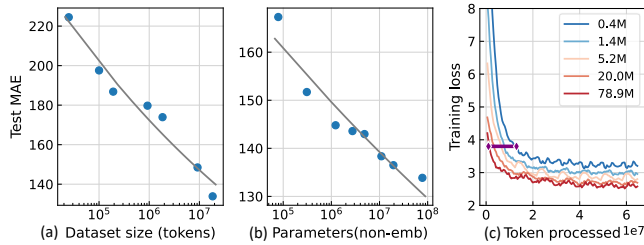
general rules among different advertising bidding scenarios, which is worthy of further exploration by the community.

6.4 Further Analysis of Bid2X

6.4.1 Ablation Study. To verify our model design, we carry out ablation experiments on the following variants: (a) **r/p va** replaces the variable attention with temporal attention. (b) **w/o va** removes the variable attention encoder. (c) **w/o ta** disables the temporal

Table 2: Ablation study on key components of our model in terms of MAE with the best in bold. Rwd: Reward. Cnt: Count.

Dataset	BCB			TR			BS			BM			BL			D6			D12			D18		
	Cost	Rwd	Cnt	Cost	Rwd	Cnt	Cost	Rwd	Cnt	Cost	Rwd	Cnt	Cost	Rwd	Cnt	Cost	Rwd	Cnt	Cost	Rwd	Cnt	Cost	Rwd	Cnt
Bid2X	122.50	5.94	12.02	172.40	8.90	13.26	148.28	7.76	14.54	751.83	31.91	47.21	4170.21	170.03	151.70	158.81	7.82	14.30	109.27	5.45	10.53	88.96	4.01	9.23
r/p va	135.06	6.39	12.73	195.39	9.86	14.28	151.91	8.08	15.27	885.30	36.13	53.23	6185.36	226.93	186.18	175.85	8.47	15.24	120.96	5.90	11.16	100.74	4.31	9.81
w/o va	150.28	6.34	13.58	219.35	9.17	15.44	169.93	8.19	16.67	1031.83	35.37	57.99	6577.34	187.51	193.17	194.41	8.34	16.13	136.83	5.72	12.06	116.66	4.35	10.91
w/o ta	159.00	7.16	17.61	227.74	10.24	19.60	178.12	9.11	21.43	1022.72	39.94	71.88	8026.04	208.97	243.45	202.42	9.43	20.65	144.70	6.45	15.64	126.72	4.80	14.50
w/o zip	138.63	8.93	14.09	198.54	12.33	15.98	160.12	11.12	16.67	900.61	44.40	60.33	5445.56	236.57	238.45	179.49	11.61	16.86	122.67	7.63	12.19	104.91	6.18	11.00
w/o cfp	131.14	6.11	12.13	188.52	9.66	13.41	150.87	7.83	14.62	846.20	33.39	49.08	5574.34	228.87	161.43	168.36	8.03	14.39	118.03	5.76	10.64	102.27	4.18	9.46

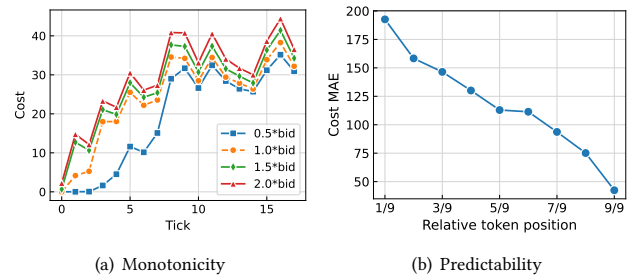
**Figure 4: Bidding environment modeling performance improves smoothly as we increase the (a) dataset size and (b) model size. (c) Training loss curve of varying-size models.**

attention modeling by padding the target entries of the decoder input as zeros. (d) **w/o zip** removes the zero-inflated projection by disabling the classification-related parts. (e) **w/o cfp** does not use the cumulative future prediction task in Eq. (14). The MAE results of all datasets are shown in Tab. 2. We can observe that all components contribute to the model’s overall performance. Specifically, variants **w/o va** and **w/o ta** show large decreases, suggesting that our proposed variable and temporal attention are indispensable for effectively and comprehensively modeling the bidding environment. Besides, the impact of removing these components on performance is more pronounced for the BL dataset compared to other datasets as its data possesses more complex relations and is more sensitive to environment modeling.

6.4.2 Scalability. Scalability is a crucial characteristic of foundation models, therefore, we explore the scaling behavior of our Bid2X *w.r.t.* dataset size D and model size N . As shown in Fig. 4(a) and (b), we observe that the model performance improves predictably as the increase of N and D , with trends spanning more than four orders of magnitude. Specifically, model performance L has a power-law relationship with each of the two scale factors N ($L = (N/3.87 \cdot 10^{75})^{-0.031}$) and D ($L = (D/3.81 \cdot 10^{38})^{-0.069}$). Moreover, as in Fig. 4(c), increasing the model parameter size accelerates the convergence of the training loss. The purple horizontal line with diamond-shaped ends demonstrates that large models have

Table 3: Monotonic ratio *w.r.t.* different cost levels.

Tick cost	(0, 0.1k]	(0.1k, 1k]	(1k, 10k]	(10k, inf)
Informer(fm)	22.42%	22.26%	22.50%	25.66%
Bid2X(fm)	82.36%	84.01%	85.44%	84.28%

**Figure 5: Our model’s adherence to physics laws.**

higher sample efficiency than small models and achieve the same level of performance with fewer processed tokens. These observations indicate that Bid2X has shown scalability behaviors, wherein larger models generally exhibit improved performance.

6.4.3 Adherence to Physics Laws. Some physical laws in ad bidding scenarios are the cornerstones of the model’s ability to generalize across different scenarios, such as monotonicity and predictability. Monotonicity refers to the fact that for a given time step of an ad campaign, the tick cost monotonically increases with the bid. Predictability refers to the fact that for a given ad campaign, the more historical bidding information is available for that day, the more predictable the next time slot’s results will be.

Firstly, we construct counterfactual samples to observe the monotonicity of the output cost by manually modifying its input control variable bid. Specifically, for each sample, we multiply its input bid by α , with α belonging to $\{0.5, 1.0, 1.5, 2.0\}$, and count the corresponding output cost during model inference. If this set of cost is monotonically increasing with the bid, then we increase the hit number by one, otherwise the missing number is increased by one. Finally, we calculate the monotonic ratio as the hit number divided by the total number, and the results are shown in Tab. 3. As observed, the monotonic ratio of our Bid2X is significantly better than Informer(fm), indicating that our model truly captures the generalized law of monotonicity through diverse training data. In addition, we randomly select an ad campaign and visualize its monotonic output. As shown in Fig. 5(a), we can see that monotonicity is satisfied throughout the execution of the ad campaign. Interestingly, the lower bid has a greater impact on cost than higher bids, indicating that the cost of obtaining ad impressions does not increase linearly.

For predictability, since bidding trajectories have different lengths, we sample 9 time slots at medium intervals for each trajectory to calculate the prediction error. The results are shown in Fig. 5(b). It

Table 4: Online A/B testing results spanning over 2 months.

	PV	Cost	BuyCnt	GMV	ROI	Latency
Bid2X vs MBRL	+7.57%	+2.16%	+3.89%	+4.65%	+2.44%	+0.05 seconds

can be found that the prediction error decreases with the increase of the historical bidding trajectory length, which indicates that our model adheres to the predictability law. Meanwhile, this also verifies the validity of the sequence information that we model by temporal attention.

6.5 Online A/B Testing Performance

Besides offline evaluation, we deploy our model on a real-world online advertising environment in Taobao, one of the largest e-commerce platforms worldwide. The platform adjusts the bid in a real-time auction system for each incoming request based on marketing values and multiple constraints imposed by advertisers. Specifically, we re-utilize the learned foundation model and settle on the bid at the $(t+1)$ -th time step corresponding to cost prediction as close to the remaining budget as possible: $b^* \in \arg \min_b |\sum_t c_t(b) - \text{budget}|$. Around one million ad campaigns set up by advertisers have been sampled for the experiment, which is a relatively small portion among all campaigns such that the auction environment is nearly stationary to any chosen campaign. We compare the adapted bidding model against model-based RL (MBRL), one of our top-performing bidding agents on the platform, in terms of the following metrics: number of page views (PV), consumed budget (Cost), the number of won impression opportunities in the episode (BuyCnt), gross merchandise value (GMV) and return on investment (ROI). As shown in Tab. 4, our model outperforms MBRL regarding the total consumed budget as well as all other metrics, which include the goal of maximizing GMV for advertisers, with only a slight increase in latency due to larger models. These improvements exhibit the effectiveness of Bid2X given the fact that the deployed bidding model requires little adjustment to the foundation model.

7 Conclusion and Future Work

This paper investigated the bidding environment modeling problem in online advertising by proposing a foundation model coined Bid2X. Specifically, we encoded heterogeneous bidding data as series embeddings and jointly captured the complex and dynamic relationships via variable and temporal attention mechanisms. We then devised a theoretically guaranteed zero-inflated projection module that combines non-zero probability estimation and value magnitude prediction to ensure the predicted value coverage of the true zero-inflated distribution. Comprehensive experiments on eight bidding datasets and online A/B tests demonstrated the generalization of Bid2X. The future work lies in (1) further improving our proposed model’s adherence to the laws of physics; (2) expanding our Bid2X to more bidding-related scenarios, e.g., campaign effectiveness prediction.

References

- [1] Muhammad Awais, Muzammal Naseer, Salman Khan, Rao Muhammad Anwer, Hisham Cholakkal, Mubarak Shah, Ming-Hsuan Yang, and Fahad Shahbaz Khan. 2023. Foundational models defining a new era in vision: A survey and outlook. *arXiv preprint arXiv:2307.13721* (2023).
- [2] Rishi Bommasani, Drew A Hudson, Ehsan Adeli, Russ Altman, Simran Arora, Sydney von Arx, Michael S Bernstein, Jeannette Bohg, Antoine Bosselut, Emma Brunskill, et al. 2021. On the opportunities and risks of foundation models. *arXiv preprint arXiv:2108.07258* (2021).
- [3] George EP Box and Gwilym M Jenkins. 1968. Some recent advances in forecasting and control. *Journal of the Royal Statistical Society. Series C (Applied Statistics)* 17, 2 (1968), 91–109.
- [4] Han Cai, Kan Ren, Weinan Zhang, Kleantlis Malialis, Jun Wang, Yong Yu, and Defeng Guo. 2017. Real-time bidding by reinforcement learning in display advertising. In *Proceedings of the 10th ACM International Conference on Web Search and Data Mining*. 661–670.
- [5] Li Chen, Penghao Wu, Kashyap Chitta, Bernhard Jaeger, Andreas Geiger, and Hongyang Li. 2024. End-to-end autonomous driving: Challenges and frontiers. *IEEE Transactions on Pattern Analysis and Machine Intelligence* (2024).
- [6] Yin Bin Cheung. 2002. Zero-inflated models for regression analysis of count data: a study of growth and development. *Statistics in medicine* 21, 10 (2002), 1461–1469.
- [7] John C Doyle, Bruce A Francis, and Allen R Tannenbaum. 2013. *Feedback control theory*. Courier Corporation.
- [8] Zhe Feng, Swati Padmanabhan, and Di Wang. 2023. Online Bidding Algorithms for Return-on-Spend Constrained Advertisers. In *Proceedings of the ACM Web Conference 2023* (Austin, TX, USA) (WWW '23). Association for Computing Machinery, 3550–3560.
- [9] Roya Firoozi, Johnathan Tucker, Stephen Tian, Anirudha Majumdar, Jiankai Sun, Weiyu Liu, Yuke Zhu, Shuran Song, Ashish Kapoor, Karol Hausman, et al. 2023. Foundation models in robotics: Applications, challenges, and the future. *The International Journal of Robotics Research* (2023), 02783649241281508.
- [10] Paul Grigas, Alfonso Lobos, Zheng Wen, and Kuang-chih Lee. 2017. Profit maximization for online advertising demand-side platforms. In *Proceedings of the ADKDD'17*. 1–7.
- [11] Nicolas Grislain, Nicolas Perrin, and Antoine Thabault. 2019. Recurrent neural networks for stochastic control in real-time bidding. In *Proceedings of the 25th ACM SIGKDD International Conference on Knowledge Discovery and Data Mining*. 2801–2809.
- [12] Jiayan Guo, Yusen Huo, Zhilin Zhang, Tianyu Wang, Chuan Yu, Jian Xu, Bo Zheng, and Yan Zhang. 2024. Generative Auto-bidding via Conditional Diffusion Modeling. In *Proceedings of the 30th ACM SIGKDD International Conference on Knowledge Discovery and Data Mining*. 5038–5049.
- [13] Yue He, Xiujun Chen, Di Wu, Junwei Pan, Qing Tan, Chuan Yu, Jian Xu, and Xiaoqiang Zhu. 2021. A unified solution to constrained bidding in online display advertising. In *Proceedings of the 27th ACM SIGKDD International Conference on Knowledge Discovery and Data Mining*. 2993–3001.
- [14] Kethmi Hirushini Hettige, Jiahao Ji, Shili Xiang, Cheng Long, Gao Cong, and Jingyuan Wang. 2024. AirPhyNet: Harnessing Physics-Guided Neural Networks for Air Quality Prediction. In *The 12th International Conference on Learning Representations*.
- [15] Charles C Holt. 2004. Forecasting seasonals and trends by exponentially weighted moving averages. *International Journal of Forecasting* 20, 1 (2004), 5–10.
- [16] Kun Hu, Shumin Zhang, Lixia Wu, Yongjun Dai, Minfang Lu, Yuting Qiang, and Minglong Li. 2025. Learning Adaptive Reserve Price in Display Advertising. In *Proceedings of the 31st ACM SIGKDD International Conference on Knowledge Discovery and Data Mining V.1*. 2282–2291.
- [17] Jiahao Ji, Jingyuan Wang, Chao Huang, Junjie Wu, Boren Xu, Zhenhe Wu, Zhang Junbo, and Yu Zheng. 2023. Spatio-Temporal Self-Supervised Learning for Traffic Flow Prediction. *Proceedings of the AAAI Conference on Artificial Intelligence* 37, 4 (2023), 4356–4364.
- [18] Jiahao Ji, Jingyuan Wang, Zhe Jiang, Jiawei Jiang, and Hu Zhang. 2022. STDEN: Towards physics-guided neural networks for traffic flow prediction. 36, 4 (2022), 4048–4056.
- [19] Jiahao Ji, Jingyuan Wang, Zhe Jiang, Jingtian Ma, and Hu Zhang. 2020. Interpretable spatiotemporal deep learning model for traffic flow prediction based on potential energy fields. In *Proceedings of the 2020 IEEE International Conference on Data Mining (ICDM'20)*. 1076–1081.
- [20] Jiahao Ji, Wentao Zhang, Jingyuan Wang, and Chao Huang. 2025. Seeing the Unseen: Learning Basis Confounder Representations for Robust Traffic Prediction. In *Proceedings of the 31st ACM SIGKDD Conference on Knowledge Discovery and Data Mining V.1*. 577–588.
- [21] Diane Lambert. 1992. Zero-inflated Poisson regression, with an application to defects in manufacturing. *Technometrics* 34, 1 (1992), 1–14.
- [22] Xu Li, Michelle Ma Zhang, Zhenya Wang, and Youjun Tong. 2022. Arbitrary distribution modeling with censorship in real-time bidding advertising. In *Proceedings of the 28th ACM SIGKDD International Conference on Knowledge Discovery and Data Mining*. 3250–3258.
- [23] Yuxuan Liang, Haomin Wen, Yuqi Nie, Yushan Jiang, Ming Jin, Dongjin Song, Shirui Pan, and Qingsong Wen. 2024. Foundation models for time series analysis: A tutorial and survey. In *Proceedings of the 30th ACM SIGKDD International Conference on Knowledge Discovery and Data Mining*. 6555–6565.

- [24] Chi-Chun Lin, Kun-Ta Chuang, Wush Chi-Hsuan Wu, and Ming-Syan Chen. 2016. Combining powers of two predictors in optimizing real-time bidding strategy under constrained budget. In *Proceedings of the 25th ACM International Conference on Information and Knowledge Management*. 2143–2148.
- [25] Jiawei Liu, Cheng Yang, Zhiyuan Lu, Junze Chen, Yibo Li, Mengmei Zhang, Ting Bai, Yuan Fang, Lichao Sun, Philip S Yu, et al. 2023. Towards graph foundation models: A survey and beyond. *arXiv preprint arXiv:2310.11829* (2023).
- [26] Xiangyu Liu, Chuan Yu, Zhilin Zhang, Zhenzhe Zheng, Yu Rong, Hongtao Lv, Da Huo, Yiqing Wang, Dagui Chen, Jian Xu, et al. 2021. Neural auction: End-to-end learning of auction mechanisms for e-commerce advertising. In *Proceedings of the 27th ACM SIGKDD International Conference on Knowledge Discovery and Data Mining*. 3354–3364.
- [27] Yong Liu, Tengge Hu, Haoran Zhang, Haixu Wu, Shiyu Wang, Lintao Ma, and Mingsheng Long. 2024. iTransformer: Inverted Transformers Are Effective for Time Series Forecasting. In *The 12th International Conference on Learning Representations*.
- [28] Yong Liu, Haixu Wu, Jianmin Wang, and Mingsheng Long. 2022. Non-stationary transformers: Exploring the stationarity in time series forecasting. *Advances in Neural Information Processing Systems* 35 (2022), 9881–9893.
- [29] Takanori Maehara, Atsuhiko Narita, Jun Baba, and Takayuki Kawabata. 2018. Optimal Bidding Strategy for Brand Advertising. In *Proceedings of the 27th International Joint Conference on Artificial Intelligence*. 424–432.
- [30] Daisuke Moriwaki, Yuta Hayakawa, Akira Matsui, Yuta Saito, Isshu Munemasa, and Masashi Shibata. 2021. A real-world implementation of unbiased lift-based bidding system. In *2021 IEEE International Conference on Big Data (Big Data)*. IEEE, 1877–1888.
- [31] Zhiyu Mou, Yusen Huo, Rongquan Bai, Mingzhou Xie, Chuan Yu, Jian Xu, and Bo Zheng. 2022. Sustainable online reinforcement learning for auto-bidding. *Advances in Neural Information Processing Systems*, 2651–2663.
- [32] Weitong Ou, Bo Chen, Xinyi Dai, Weinan Zhang, Weiwen Liu, Ruiming Tang, and Yong Yu. 2023. A survey on bid optimization in real-time bidding display advertising. *ACM Transactions on Knowledge Discovery from Data* 18, 3 (2023), 1–31.
- [33] Syama Sundar Rangapuram, Matthias W Seeger, Jan Gasthaus, Lorenzo Stella, Yuyang Wang, and Tim Januschowski. 2018. Deep state space models for time series forecasting. In *Advances in Neural Information Processing Systems*. 7796–7805.
- [34] Kan Ren, Jiarui Qin, Lei Zheng, Zhengyu Yang, Weinan Zhang, and Yong Yu. 2019. Deep landscape forecasting for real-time bidding advertising. In *Proceedings of the 25th ACM SIGKDD International Conference on Knowledge Discovery and Data Mining*. 363–372.
- [35] Kan Ren, Weinan Zhang, Ke Chang, Yifei Rong, Yong Yu, and Jun Wang. 2017. Bidding machine: Learning to bid for directly optimizing profits in display advertising. *IEEE Transactions on Knowledge and Data Engineering* 30, 4 (2017), 645–659.
- [36] Jürgen Schmidhuber, Sepp Hochreiter, et al. 1997. Long short-term memory. *Neural Computing* 9, 8 (1997), 1735–1780.
- [37] Jingyuan Wang, Jiahao Ji, Zhe Jiang, and Leilei Sun. 2023. Traffic Flow Prediction Based on Spatiotemporal Potential Energy Fields. *IEEE Transactions on Knowledge and Data Engineering* 35, 9 (2023), 9073–9087.
- [38] Jingyuan Wang, Honghao Shi, Jiahao Ji, Xin Lin, and Huaiyu Tian. 2023. High-Resolution Data on Human Behavior for Effective COVID-19 Policy-Making—Wuhan City, Hubei Province, China, January 1–February 29, 2020. *China CDC Weekly* 5, 4 (2023), 76–81.
- [39] Jun Wang, Weinan Zhang, Shuai Yuan, et al. 2017. Display advertising with real-time bidding (RTB) and behavioural targeting. *Foundations and Trends in Information Retrieval* 11, 4-5 (2017), 297–435.
- [40] Chao Wen, Miao Xu, Zhilin Zhang, Zhenzhe Zheng, Yuhui Wang, Xiangyu Liu, Yu Rong, Dong Xie, Xiaoyang Tan, Chuan Yu, et al. 2022. A cooperative-competitive multi-agent framework for auto-bidding in online advertising. In *Proceedings of the Fifteenth ACM International Conference on Web Search and Data Mining*. 1129–1139.
- [41] Qingsong Wen, Tian Zhou, Chaoli Zhang, Weiqi Chen, Ziqing Ma, Junchi Yan, and Liang Sun. 2023. Transformers in time series: a survey. In *Proceedings of the 32nd International Joint Conference on Artificial Intelligence*. 6778–6786.
- [42] Haixu Wu, Jiehui Xu, Jianmin Wang, and Mingsheng Long. 2021. Autoformer: Decomposition transformers with auto-correlation for long-term series forecasting. *Advances in Neural Information Processing Systems* 34 (2021), 22419–22430.
- [43] Ailing Zeng, Muxi Chen, Lei Zhang, and Qiang Xu. 2023. Are transformers effective for time series forecasting?. In *Proceedings of the AAAI conference on artificial intelligence*, Vol. 37. 11121–11128.
- [44] Weinan Zhang, Yifei Rong, Jun Wang, Tianchi Zhu, and Xiaofan Wang. 2016. Feedback control of real-time display advertising. In *Proceedings of the 9th ACM International Conference on Web Search and Data Mining*. 407–416.
- [45] Weinan Zhang, Ying Zhang, Bin Gao, Yong Yu, Xiaojie Yuan, and Tie-Yan Liu. 2012. Joint optimization of bid and budget allocation in sponsored search. In *Proceedings of the 18th ACM SIGKDD International Conference on Knowledge Discovery and Data Mining*. 1177–1185.
- [46] Yunhao Zhang and Junchi Yan. 2023. Crossformer: Transformer utilizing cross-dimension dependency for multivariate time series forecasting. In *The 11th International Conference on Learning Representations*.
- [47] Wayne Xin Zhao, Kun Zhou, Junyi Li, Tianyi Tang, Xiaolei Wang, Yupeng Hou, Yingqian Min, Beichen Zhang, Junjie Zhang, Zican Dong, et al. 2023. A survey of large language models. *arXiv preprint arXiv:2303.18223* (2023).
- [48] Xiangyu Zhao, Long Xia, Jiliang Tang, and Dawei Yin. 2019. Deep reinforcement learning for search, recommendation, and online advertising: a survey. *ACM Sigweb Newsletter* 2019, Spring (2019), 1–15.
- [49] Haoyi Zhou, Shanghang Zhang, Jieqi Peng, Shuai Zhang, Jianxin Li, Hui Xiong, and Wancai Zhang. 2021. Informer: Beyond efficient transformer for long sequence time-series forecasting. In *Proceedings of the AAAI conference on artificial intelligence*, Vol. 35. 11106–11115.
- [50] Tian Zhou, Ziqing Ma, Qingsong Wen, Xue Wang, Liang Sun, and Rong Jin. 2022. Fedformer: Frequency enhanced decomposed transformer for long-term series forecasting. In *International conference on machine learning*. PMLR, 27268–27286.
- [51] Yunhong Zhou, Deeparnab Chakrabarty, and Rajan Lukose. 2008. Budget constrained bidding in keyword auctions and online knapsack problems. In *Proceedings of the 17th International Conference on World Wide Web*. 1243–1244.
- [52] Han Zhu, Junqi Jin, Chang Tan, Fei Pan, Yifan Zeng, Han Li, and Kun Gai. 2017. Optimized cost per click in taobao display advertising. In *Proceedings of the 23rd ACM SIGKDD International Conference on Knowledge Discovery and Data Mining*. 2191–2200.

A Technical Proofs

Theorem 3 (Zero-inflated Proper Loss). *Let \mathcal{F} be a set of all measurable functions and $p_\theta, g_\phi \in \mathcal{F}$. Assume that p and g are conditionally independent, then, with respect to the zero-inflated model defined in Eq. (16), we have $p_{\theta^*}(\mathbf{x}) = p(\mathbf{x})$ and $p_{\theta^*}(\mathbf{x})g_{\phi^*}(\mathbf{x}) = p(\mathbf{x})g(\mathbf{x})$, therefore $f(\mathbf{x}) = \mathbb{E}[Y|\mathbf{x}]$ for any $\mathbf{x} \in \mathbb{R}^d$. In addition, $g_{\phi^*}(\mathbf{x})$ is generally not unique.*

PROOF. Since p and g are conditionally independent, by taking the expectation over Y , the objective can be rewritten as

$$\min_{\theta, \phi} \mathbb{E}_{X \sim \mathbb{P}} (p_\theta(X)g_\phi(X) - p(X)g(X))^2 + H(p(X)|p_\theta(X)).$$

Furthermore, based on the i. i. d. assumption, it is straightforward to focus on solving the sub-problem for each X independently:

$$\min_{\theta, \phi} (p_\theta g_\phi - pg)^2 + H(p|p_\theta),$$

where we omit the dependency on X for ease of notation.

The stationarity conditions of p_θ and g_ϕ suggest that

$$\frac{\partial}{\partial p_\theta} \ell = 2g_\phi(p_\theta g_\phi - pg) - \frac{p}{p_\theta} + \frac{1-p}{1-p_\theta} = 0$$

$$\frac{\partial}{\partial g_\phi} \ell = 2p_\theta(p_\theta g_\phi - pg) = 0,$$

which yields the solution $p_{\theta^*} = p$ and $p_{\theta^*}g_{\phi^*} = pg$ for $p_{\theta^*} \in (0, 1)$. This is applicable to the cases where $p_\theta \in \{0, 1\}$ when $p \in \{0, 1\}$ respectively because otherwise the entropy term would be ∞ . Thereafter, the optimality conditions hold for $p_{\theta^*} \in [0, 1]$. According to the assumption that p_θ and g_ϕ could be any measurable functions, the optimality conditions are satisfiable.

However, optimizing \mathcal{L} does not guarantee a unique g_{ϕ^*} due to its non-convexity. This conclusion follows directly from the observation of its Hessian matrix:

$$H_\ell := \begin{bmatrix} 2g_\phi^2 + \frac{p}{p_\theta} + \frac{(1-p_\theta)}{(1-p_\theta)^2} & 4p_\theta g_\phi - 2pg \\ 4p_\theta g_\phi - 2pg & 2p_\theta^2 \end{bmatrix}.$$

Table 5: Basic information of all datasets.

Dataset	Description	# Records	# Trajectories
BCB	Data in budget constrained bidding scenarios	47,879,102	1,128,142
TR	Data in target ROAS scenarios	7,601,466	187,030
BS	Data of small-budget advertisers with the budget in (0, 5000]	21,268,728	521,240
BM	Data of middle-budget advertisers with the budget in (5000, 50000]	3,353,924	78,426
BL	Data of large-budget advertisers with the budget (50000, inf)	136,520	2,934
D6	Data with ad delivery duration of 6-12 hours	22,308,744	643,386
D12	Data with ad delivery duration of 12-18 hours	23,541,560	425,948
D18	Data with ad delivery duration of 18-24 hours	6,644,174	83,762

We know that $p_{\theta^*} = p$. Let $g_\phi = ag$ for some $a \in \mathbb{R}$. Furthermore, let $a > \frac{2}{3} + \sqrt{\frac{1}{9} + \frac{1}{6pg^2(1-p)}}$. The determinant therefore satisfies

$$H_\ell = \frac{p}{1-p} [(-12a^2 + 16a - 4)pg^2(1-p) + 2] < 0.$$

The objective is thus non-convex for $p_\theta, g_\theta \in [0, 1]$. \square

B Experimental Settings

B.1 Datasets

Here we provide more details of the datasets used in our study. We collect various bidding data from multiple scenarios and advertiser types. Tab. 5 summarizes the basic information of the used datasets, and Tab. 6 reports the basic statistics.

Table 6: Statistics of datasets.

Dataset	Bid		Cost		Reward		Count	
	Mean	SD	Mean	SD	Mean	SD	Mean	SD
BCB	216.18	468.37	212.92	1068.67	10.00	65.20	25.15	101.25
TR	153.29	150.90	314.47	1417.75	15.42	180.82	28.85	103.65
BS	96.17	162.71	233.58	491.87	12.08	58.22	30.71	85.41
BM	172.38	288.93	1423.41	2475.33	61.95	221.72	104.97	278.37
BL	331.16	443.08	9800.88	13929.62	351.39	1148.51	372.36	689.95
D6	174.80	161.20	281.18	1307.49	13.48	87.47	29.60	116.15
D12	184.66	278.02	181.47	945.31	8.68	95.23	22.17	86.20
D18	220.97	331.04	140.56	762.13	5.77	38.36	19.14	77.93

B.2 Baselines

We compare our Bid2X with 9 baselines as follows:

- **DLF** [34]: is a classic landscape forecasting model utilizing RNN-based approach.
- **ADM** [22]: is a recent landscape forecasting literature, which devises a novel neighborhood likelihood loss for arbitrary distribution modeling.
- **LP** [13]: a heuristic method that utilizes linear programming to solve the environment by using historical bidding records, which may not match the current bidding environment due to its dynamic property.
- **MMP** [26]: a min-max predictor that can ensure the partial monotonicity between the control variables and target variables, which is a widely-used model in bidding scenarios.

- **MLP** [12]: a common environment model in model-based reinforcement learning for auto-bidding. It can directly learn the relations between control variables and target variables, but it neglects the sequence information inherent in bidding trajectories.
- **iTransformer** [27]: a variable-based approach that takes each variable’s series as a token and feeds it into a standard Transformer model. Since today’s bidding data is not complete, we use historical bidding data that is complete as input.
- **non-stationary transformer (NST)** [28]: a temporal-based series prediction approach aiming for the inherent non-stationarity problem, which is very common in bidding data.
- **Informer** [49]: a temporal-based transformer model tailored for long-term series forecasting.
- **Informer(fm)**: we train Informer in a one-for-all foundation paradigm for fair comparison.

All baselines are separately trained on each dataset to learn a dedicated model except Informer(fm). The baseline Informer(fm) is trained on all datasets similar to our Bid2X.

C Few-shot Performance

Tab. 7 reports the few-shot learning results.

Table 7: Few-shot performance of Bid2X and baselines *w.r.t.* MAE. The bold/underlined font means the best/the second-best result.

Task	Few-shot (1%)			Few-shot (5%)		
	Cost	Reward	Count	Cost	Reward	Count
MLP	59.66	3.59	58.58	58.68	3.40	58.29
iTransformer	68.64	3.48	64.06	67.48	3.50	65.01
NST	65.25	3.50	61.95	61.08	3.29	56.69
Informer(fm)	54.34	3.20	56.83	<u>51.41</u>	3.18	55.80
Bid2X(fm)	45.63	2.65	38.09	43.50	2.55	36.76

D Impact of Hyperparameters

In this part, we conduct experiments to analyze the impacts of critical hyperparameters: the number of layers, the hidden dimension, and the balancing factor. In Fig. 6, we present the MAE results on the mixed dataset with different parameters.

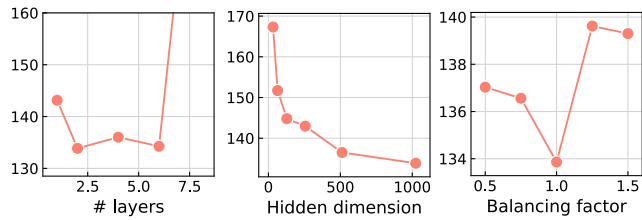


Figure 6: Parameter sensitivity of Bid2X using MAE metric.

Firstly, we keep the encoder and decoder layers the same and vary them in the set $\{1, 2, 4, 6, 8\}$. The results indicate that 2 and 6 deliver similar results. Considering the computation cost, we choose 2 as the final setting. Secondly, the hidden dimension is adjusted in the set $\{32, 64, 128, 256, 512, 1024\}$. The results indicate 1024 as the optimal setting. Although the performance can increase with a larger dimensionality, we use 1024 since it can produce satisfactory performance. Thirdly, the effect of the balancing factor is tested in $\{0.5, 0.75, 1.0, 1.25, 1.5\}$. We can observe that a setting of 1.0 is optimal for our model.

E Distribution Visualization

In this part, we inspect the distribution of our model’s prediction, to verify that our proposed zero-inflated projection can ensure

the predicted data converges to the zero-inflated distribution. We visualized the learned distribution for the cost variable in Fig. 7. The results demonstrate that the cost predicted by our Bid2X is consistent with the zero-inflated distribution. However, the baseline Informer that uses the classic neural network objective function converges to a normal distribution, which is inconsistent with the true bidding data distribution.

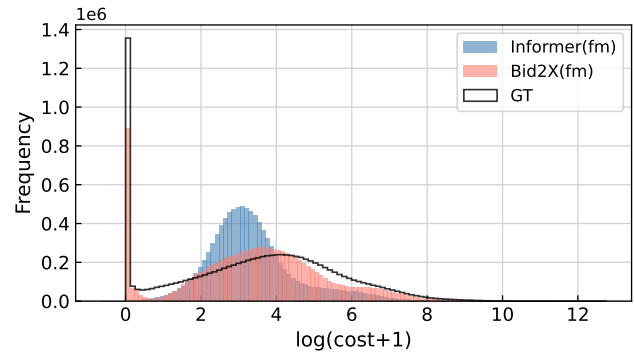


Figure 7: Distribution of cost prediction. GT: Ground Truth.